

# Significant improvement of electrochemical performance of Cu-coated $\text{LiVPO}_4\text{F}$ cathode material for lithium-ion batteries

YU ZHANG<sup>a,\*</sup>, XIAOLAN BAI<sup>b</sup> and CUILING LI<sup>a</sup>

<sup>a</sup>School of Mechanical Engineering and Automation, Northeastern University, Shenyang 110819, China

<sup>b</sup>School of Mechanical Engineering, Shenyang University of Chemical Technology, Shenyang 110142, China  
e-mail: zy4097534@126.com

MS received 17 January 2015; revised 15 April 2015; accepted 14 May 2015

**Abstract.** In this paper, we reveal that the intrinsic low electronic conductivity of the pristine  $\text{LiVPO}_4\text{F}$  is overcome with conductive Cu-coating. The existence of nano-Cu is confirmed with X-ray diffraction (XRD) and energy dispersive spectroscopy (EDS). The morphology and particle size are observed by scanning electron microscopy (SEM). Galvanostatic charge/discharge test indicates that Cu coating is effective to improve the discharge capacity, cycle performance and rate capability. Analysis of electrochemical impedance spectra (EIS) shows that the addition of nano-Cu markedly decreases the charge transfer resistance of the pristine  $\text{LiVPO}_4\text{F}$  electrode.

**Keywords.** Lithium-ion batteries; cathode material;  $\text{LiVPO}_4\text{F}$ ; surface modification.

## 1. Introduction

The storage of electrical energy at high charge and discharge rate is an important technology in society.<sup>1</sup> Lithium-ion batteries are considered the most advanced electrical energy storage and transfer systems. Cathode material is one of the crucial factors that determine the electrochemical performance of lithium-ion batteries. As a new high-voltage cathode material, triclinic structured  $\text{LiVPO}_4\text{F}$  which was first reported by Barker<sup>2–4</sup> has been developed in recent years as a promising candidate for next-generation cathode material due to its environmental safety, long life cycle and high energy density. It is isostructural with the naturally-occurring mineral tavorite,  $\text{LiFePO}_4\cdot\text{OH}$  or ambylgonite,  $\text{LiAlPO}_4\text{F}$  and crystallizes with a triclinic structure (space group P).<sup>5</sup> Besides, it has a relatively high potential of 4.2 V (vs.  $\text{Li}^+/\text{Li}$ ) and a theoretical capacity of  $156 \text{ mAh g}^{-1}$  based on the extracted  $\text{Li}^+$  ion from the material lattice. Unlike other 4 V cathode materials,<sup>6–8</sup>  $\text{LiVPO}_4\text{F}$  shows excellent lattice stability and good thermal stability with electrolyte owing to the consolidus covalent-bonded crystal structure.

Unfortunately, the electronic conductivity of the pristine  $\text{LiVPO}_4\text{F}$  electrode is poor, which is an intrinsic drawback to its electrochemical performance. In

order to resolve this stringent shortcoming, it is a common practice to prepare carbon coated materials.<sup>9,10</sup> Zhou *et al.*<sup>9</sup> synthesized  $\text{LiVPO}_4\text{F}/\text{C}$  cathode material via a sol-gel method followed by low temperature calcination and reported a discharge capacity of about  $130 \text{ mAh g}^{-1}$  at  $30 \text{ mA g}^{-1}$  in the range of 3.0–4.6 V at the first cycle. Another simple surface modification strategy to enhance the electronic conductivity of the pristine cathode is coating the particles with conductive metal material. For instance, Wang *et al.*<sup>11</sup> increased the initial discharge capacity of  $\text{Li}_3\text{V}_2(\text{PO}_4)_3$  from 132 to  $160 \text{ mAh g}^{-1}$  by adding of 1.8 wt% Cu powder into the precursor solution. Moreover, this approach was also successfully adapted to some other cathode materials ( $\text{LiFePO}_4$ )<sup>12</sup>.

To our knowledge, improvement is not reported in the electrochemical performance of  $\text{LiVPO}_4\text{F}$  by Cu coating. Therefore, in this work, we synthesized  $\text{LiVPO}_4\text{F}/\text{Cu}$  using the precursor obtained via a soft chemical route with mechanical activation assistance. The electrochemical performance of the surface-treated material is compared and discussed with that of the pristine  $\text{LiVPO}_4\text{F}$  material.

## 2. Experimental

The pristine  $\text{LiVPO}_4\text{F}$  sample was synthesized using the precursor obtained via a soft chemical route with

\*For correspondence

mechanical activation assistance described by Wang *et al.*<sup>10</sup>  $V_2O_5$ ,  $NH_4H_2PO_4$ , LiF and 5% excess oxalic acid were used as the raw materials. Firstly, the raw materials were ground in an agate mortar. Secondly, the homogeneous mixture reacted under ball milling for 5 h in ethanol media at room temperature, with a revolving speed of 400 rpm. After that, the obtained slurry was dried at 80°C for 12 h to evaporate the ethanol. Finally, the precursor was annealed at 300°C for 4 h, and then sintered at 650°C for 6 h in a tubular furnace under  $N_2$  atmosphere.

The Cu (2 wt%)-coated  $LiVPO_4F$  cathode material was synthesized as follows.  $LiVPO_4F$  powder was firstly suspended in absolute ethyl alcohol with vigorous stirring. Then the  $Cu(NO_3)_2 \cdot 3H_2O$  with a weight ratio of 2(Cu):98( $LiVPO_4F$ ) was added. After stirring for 30 min, the solution of ascorbic acid was slowly added to the mixture. The suspended powder was separated by a centrifugal separator and then dried at 90°C for 12 h. Finally, the obtained product was calcined at 650°C for 2 h in a tubular furnace under  $N_2$  atmosphere to obtain the  $LiVPO_4F/Cu$  sample

The phase identification of the pristine and Cu-coated  $LiVPO_4F$  samples was analyzed by XRD (Rigaku MiniFlexII) using Cu  $K\alpha$  radiation ( $\lambda = 0.15405$  nm). The morphology of the as-synthesized samples was studied with a SEM (JSM-7500F, Japan) equipped with an EDS.

The charge/discharge behavior of the obtained samples was examined using CR2025 coin-type cells. The working electrode was prepared by homogeneously pasting a slurry containing 85 wt% active material, 10 wt% super P and 5 wt% PVDF dissolved in NMP on an Al foil and subsequently dried in the vacuum oven at 120°C for 12 h. The coin cells were assembled in a glove box filled with argon gas. Li metal was used as anode and Celgard 2300 film was used as separator. The electrolyte used was  $LiPF_6$  ( $1 \text{ mol L}^{-1}$ ) in a mixture of ethylene carbonate (EC) and dimethyl carbonate (DMC) (1:1 in vol. ratio). Galvanostatic charge/discharge cycling tests were carried out between 3.0 and 4.5 V using a land CT2001 tester (Wuhan, China). EIS was performed in the frequency range from 0.01 to 100 kHz by an electrochemical working station (Shanghai Chenhua Instrument Co. Ltd., China). All tests were carried out at room temperature.

### 3. Results and Discussion

Figure 1 shows the XRD patterns of the pristine and Cu-coated  $LiVPO_4F$  samples synthesized under the same process. It can be seen that all of the peaks can be

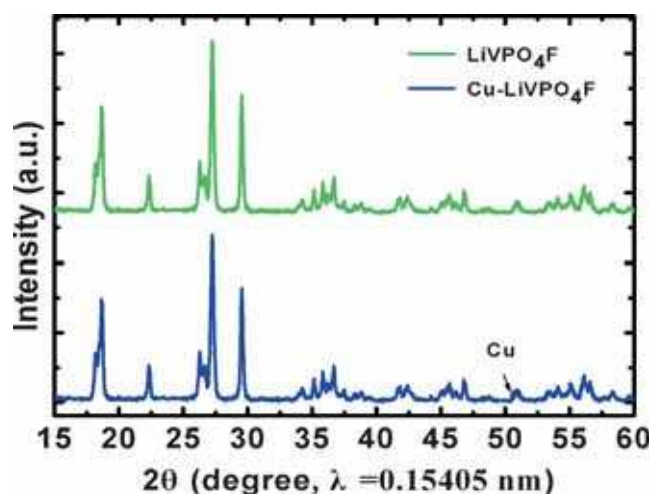


**Figure 1.** XRD patterns of  $LiVPO_4F$  and  $LiVPO_4F/Cu$  powders.

identified as  $LiVPO_4F$  with an ordered triclinic structure indexed to space group  $p$  (JCPDS card No. 42-1412), which are similar to the previously reported papers.<sup>3,10,13</sup> Besides, no unexpected impurity peaks such as  $V_2O_3$  or LiF are observed in the XRD patterns of both the pristine and Cu-coated  $LiVPO_4F$ , indicating uniform mixing of raw materials during ball milling and completion of expected reaction from Li-V- $PO_4$ -F to crystal  $LiVPO_4F$ .

The morphologies of the  $LiVPO_4F$  powder before and after Cu coating are shown in figure 2. It can be found that both the pristine and Cu-coated  $LiVPO_4F$  particles are about hundreds of nanometers in size, which is much smaller than those synthesized by conventional solid-state reaction.<sup>14,15</sup> What is more, there is no obvious difference on morphology and particle size distribution between the two samples, implying that Cu coating has little effect on the morphology of  $LiVPO_4F$  particles.

In order to clearly confirm the presence of Cu particles on the surface of  $LiVPO_4F$  sample, EDS dot mapping of Cu element was carried out (figure 3). Through the EDX mapping, it can be observed that the Cu is uniformly distributed without aggregation, giving unequivocal evidence to the presence of Cu coating on the surface of  $LiVPO_4F$  particles.

The typical TEM image of Cu-coated  $LiVPO_4F$  is shown in figure 4. It can be seen that there are two different kinds of particles which correspond to the  $LiVPO_4F$  and Cu particles. The nanosized Cu particles with average diameter of 10 nm are uniformly dispersed on the surface of  $LiVPO_4F$  sample. It should be noticed that the Cu particles are segregated as second phase in the sample.

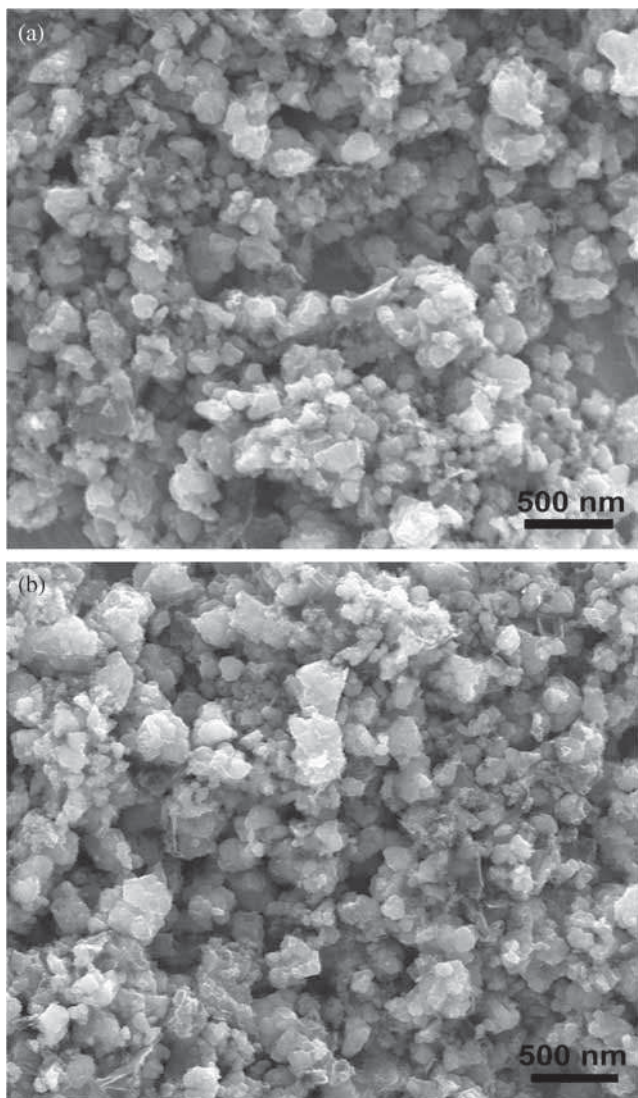


**Figure 2.** SEM images of (a) pristine and; (b) Cu-coated  $\text{LiVPO}_4\text{F}$  particles.

Figure 5 shows the Cu XPS core level for  $\text{LiVPO}_4\text{F}/\text{Cu}$  sample. According to figure 5, it can be seen that the binding energy of Cu  $2p_{3/2}$  is 932.6 eV with a difference of 19.7 eV between Cu  $2p_{1/2}$ . Since Cu was determined by XPS and no Cu-based impurity was detected by XRD (figure 1), Cu is anticipated to be successfully coating the surface of  $\text{LiVPO}_4\text{F}$  particles.

Figure 6 a,b shows the initial charge/discharge curves of the pristine and Cu-coated  $\text{LiVPO}_4\text{F}$  at 0.01 C and 0.2 C between 3.0 and 4.5 V. The charge/discharge profiles exhibit a charge plateau around 4.3 V and discharge plateau around 4.2 V, corresponding to the  $\text{V}^{3+}/\text{V}^{4+}$  redox reaction.<sup>9</sup> The pristine  $\text{LiVPO}_4\text{F}$  presents discharge capacities of 122.5 and 106.6  $\text{mAh g}^{-1}$  at 1/100 and 0.2 C for the first cycle,

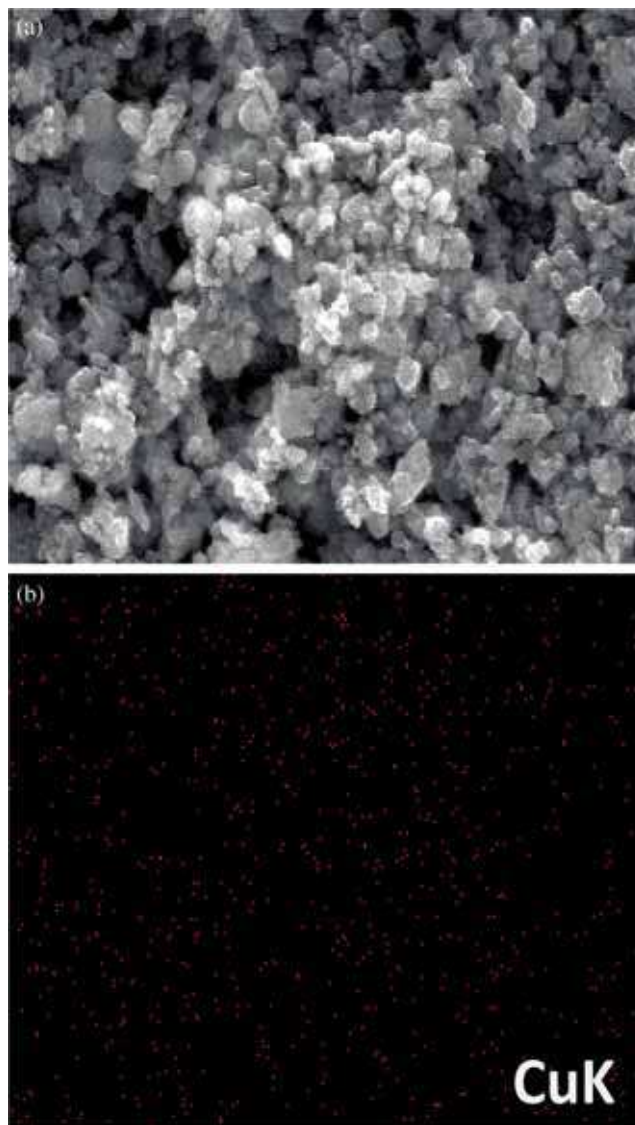


**Figure 3.** (a) SEM image of  $\text{LiVPO}_4\text{F}/\text{Cu}$  and; (b) the corresponding EDS dot mapping of Cu element.

respectively. The low capacity of the pristine sample is due to the relatively low electronic conductivity and low diffusion rate of  $\text{Li}^+$  ions within the structure, which limits the amount of  $\text{Li}^+$  ions that can be extracted. After Cu modification, the sample shows high discharge capacities of 145.3 and 125.8  $\text{mAh g}^{-1}$  at 0.01 and 0.2 C, respectively. The improved electrochemical performance is attributed to the higher electronic conductivity and better ionic conductivity owing to the stability of the  $\text{LiVPO}_4\text{F}/\text{Cu}$  particles by addition of Cu. In a word, Cu could ameliorate the electrical performance of the  $\text{LiVPO}_4\text{F}/\text{Cu}$  during the charge/discharge process. The cycle performances of the two samples at 0.2 C are given in figure 6(c). The discharge capacity of the pristine sample decreases gradually with

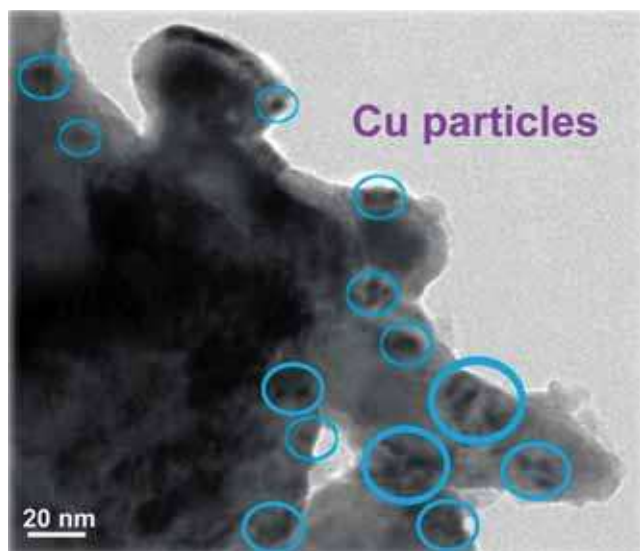


Figure 4. TEM image of Cu-coated LiVPO<sub>4</sub>F sample.

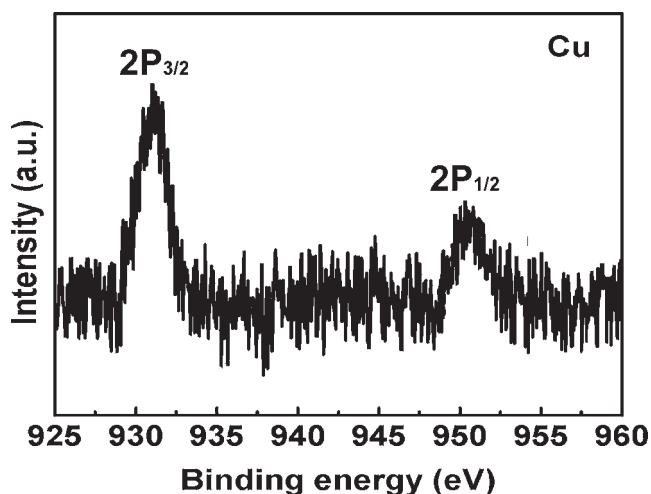


Figure 5. XPS spectrum of Cu<sub>2p</sub> in the LiVPO<sub>4</sub>F/Cu sample.

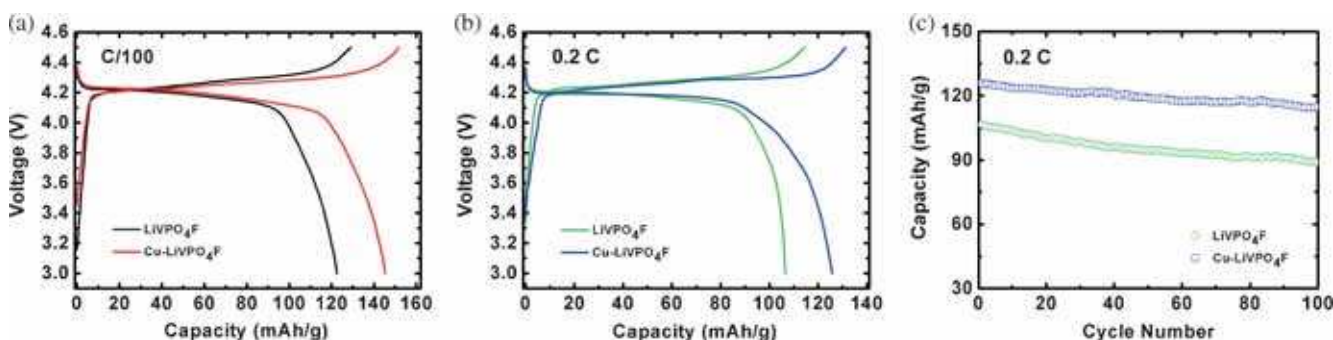
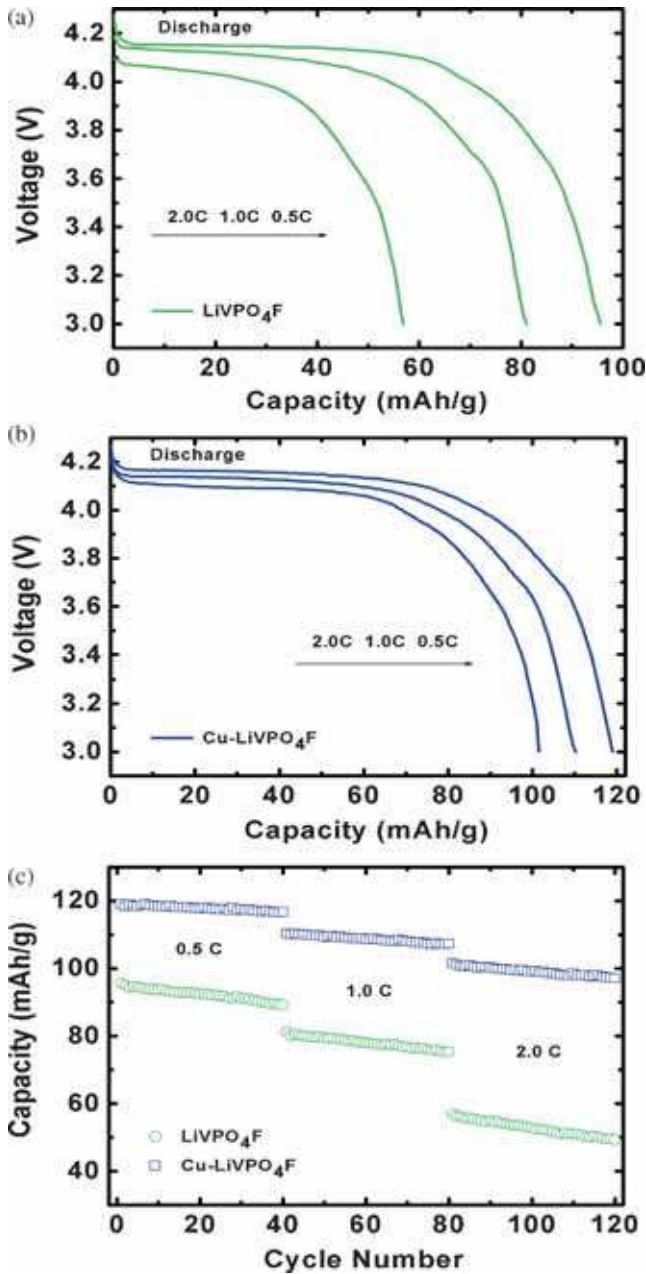


Figure 6. (a, b) Initial charge/discharge curves and; (c) cycle performances of LiVPO<sub>4</sub>F and LiVPO<sub>4</sub>F/Cu electrodes at C/100 or 0.2 C between 3.0 V and 4.5 V.

cycling and finally reaches 83.5% of its initial discharge capacity after 100 cycles. On the contrary, when the LiVPO<sub>4</sub>F was coated with conductive Cu, the cycle-life retention was improved to 91.1% of its initial discharge capacity. It is evident that Cu coating can significantly improve the cycle performance of LiVPO<sub>4</sub>F electrode.

Figure 7 displays the rate capability of the pristine and Cu-coated LiVPO<sub>4</sub>F in the voltage range of 3.0–4.5 V. It is obvious from figure 7(a) that the coated sample clearly shows a better rate capability than the pristine sample. For both the samples, the charge/discharge capacities exhibit a tendency to decrease with increasing current density, which is similar to the previous work.<sup>16</sup> Moreover, as the charge/discharge rate increases, the LiVPO<sub>4</sub>F/Cu cathode presents a slower enlargement in electrochemical polarization. Lower polarization suggests better reaction kinetics. Figure 7(b) compares the cycle performances of the as-synthesized cathodes. At a rate of 0.5 C, the Cu-modified cathode shows a discharge capacity of 116.6 mAh g<sup>-1</sup> after 40 cycles. However, the capacity retention of the pristine cathode maintains 93.2% of its initial discharge capacity, lower than 98.1% delivered by the Cu-modified sample, and this gap is more obvious at high rates. From the above analysis, it can be concluded that the electronic conductivity between active materials is enhanced by surface modification with Cu, which consequently results in superior rate capability of the cells.

EIS measurements were carried out on the pristine and Cu-coated LiVPO<sub>4</sub>F electrodes. The typical Nyquist plots and equivalent circuit<sup>17</sup> are shown in figure 8. It is clear that the plots show an intercept at high frequency, followed by a depressed semi-circle in the high-middle frequency region and a straight line in the low frequency region. The intercept impedance on the Z' axis represents the resistance of



**Figure 7.** Rate capability of pristine LiVPO<sub>4</sub>F (a) and Cu-coated LiVPO<sub>4</sub>F; (b) from 0.5 C to 2.0 C in the voltage range of 3.0 V–4.5 V; (c) cycle performances of the two samples for 40 cycles.

solvent. The high frequency semicircle is related to the charge-transfer resistance ( $R_{ct}$ ), and the line indicates the Warburg impedance, which is attributed to the diffusion of Li<sup>+</sup> in the electrode.<sup>18</sup> According to figure 8, it can be seen that the charge-transfer resistance of Cu-coated LiVPO<sub>4</sub>F electrode is much smaller than that of the pristine LiVPO<sub>4</sub>F, indicating that the electronic conductivity between LiVPO<sub>4</sub>F particles is enhanced due to the presence of Cu coating. This result is similar to that of Cu-coated Li<sub>3</sub>V<sub>2</sub>(PO<sub>4</sub>)<sub>3</sub>.<sup>11</sup>

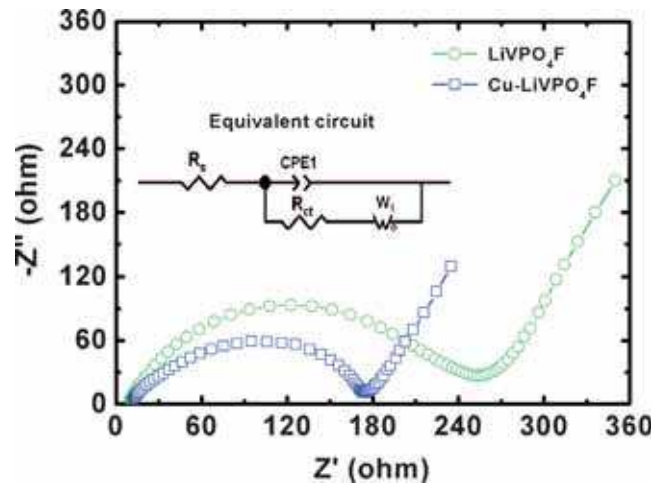


**Figure 8.** Nyquist plots of LiVPO<sub>4</sub>F and LiVPO<sub>4</sub>F/Cu electrodes with testing frequency from 0.01 Hz to 100 kHz. Inset: the equivalent circuit model.

#### 4. Conclusions

Nano-Cu coating on the surface of the pristine LiVPO<sub>4</sub>F particles was successfully synthesized for the first time via a soft chemical route with mechanical activation assistance. The effect of Cu coating on the crystalline structure, morphology and electrochemical performance of the samples have been investigated in detail. XRD results show that the Cu modification does not affect the triclinic structure of LiVPO<sub>4</sub>F sample. EDS dot mapping reveals that the Cu is uniformly distributed on the surface of LiVPO<sub>4</sub>F particles. Cu-coated LiVPO<sub>4</sub>F cathode material exhibits improved electrochemical performance relative to the pristine LiVPO<sub>4</sub>F. The initial discharge capacity is increased from 106.6 mAh g<sup>-1</sup> for pristine LiVPO<sub>4</sub>F to 125.8 mAh g<sup>-1</sup> for LiVPO<sub>4</sub>F/Cu at 0.2 C. Moreover, the Cu-coated LiVPO<sub>4</sub>F can still deliver a discharge capacity of 101.5 mAh g<sup>-1</sup> at a rate of 2.0 C, and sustain 95.7% of capacity retention after 40 cycles. EIS indicates that the charge transfer resistance of the pristine LiVPO<sub>4</sub>F cell shifts from 253 Ω to 175 Ω after Cu coating. The better electrochemical performance of LiVPO<sub>4</sub>F with 2 wt% Cu coating can be contributed to the higher electronic conductivity and better ionic conductivity among particles.

#### Acknowledgement

This project was supported by National Natural Science Foundation of China (Grant No. 51205054), Research Fund for Talents of Northeastern University (Grant No. 26333002), Liaoning Province Enterprise Postdoctoral Funded Project and China Postdoctoral Science Foundation funded project (Grant No. 2014M551106).

**References**

1. Goodenough J B 2007 *J. Power Sources* **174** 996
2. Barker J, Saidi M Y and Swoyer J L 2004 *J. Electrochem. Soc.* **151** A1670
3. Barker J, Gover P K B, Bryan A and Saidi M Y 2005 *J. Power Sources* **146** 516
4. Gover P K B, Burns P, Bryan A, Saidi M Y, Swoyer J L and Barker J 2006 *Solid State Ionics* **177** 2635
5. Barker J Saidi M Y and Swoyer J L 2003 *J. Electrochem. Soc.* **150** A1394
6. Thackeray M M, Johnson P J, de Picciotto L A, Bruce P G and Goodenough J B 1984 *Mater. Res. Bull.* **19** 179
7. Koksang R, Barker J, Shi H and Saidi M Y 1996 *Solid State Ionics* **84** 1
8. Pivko M, Bele M, Tchernychova E, Logar N Z, Dominko R and Gaberscek M 2012 *Chem. Mater.* **24** 1041
9. Li Y Z, Zhou Z, Gao X P and Yan J 2006 *J. Power Sources* **160** 633
10. Wang J X, Li X H, Wang Z X, Guo H J, Zhang Y H, Xiong X H and He Z J 2013 *Electrochim. Acta* **91** 75
11. Jiang T, Wei Y J, Ming X, Chen G and Wang C Z 2009 *J. Alloys Compd.* **488** L26
12. Croce F, Epifanio A D, Hassoun J, Deptula A, Olczac T and Scrosati B 2002 *Electrochem. Solid-State Lett.* **5** A47
13. Ma R, Shu J, Shao L Y, Lin X T, Wu K Q, Shui M, Li P, Long N B and Ren Y L 2014 *Ceram. Int.* **40** 15113
14. Zhong S K, Yin Z L, Wang Z X and Chen Q Y 2007 *J. Cent. S. Univ. Technol.* **14** 340
15. Li Y Z, Ren J X, Zhou Z, Gao X P and Yan J 2005 *Chin. J. Inorg. Chem.* **21** 1597
16. Zhang Q, Zhong S K, Liu L T, Liu J Q, Jiang J Q, Wang J and Li Y H 2009 *J. Phys. Chem. Solids* **70** 1080
17. Wang G X, Yang L and Chen Y 2005 *Electrochim. Acta* **50** 4649
18. Gao F and Tang Z 2008 *Electrochim. Acta* **53** 5071